Networked and Distributed Control Method with Optimal Power Dispatch for Islanded Microgrids

Li, Qiang; Peng, Congbo; Chen, Minyou; Chen, Feixiong; Kang, Wenfa; Guerrero, Josep M.; Abbott, Derek

Published in:
I E E E Transactions on Industrial Electronics

DOI (link to publication from Publisher):
10.1109/TIE.2016.2598799

Publication date:
2017

Document Version
Early version, also known as pre-print

Networked and Distributed Control Method with Optimal Power Dispatch for Islanded Microgrids

Qiang Li, Congbo Peng, Minyou Chen, *Senior Member*, *IEEE*, Feixiong Chen, Wenfa Kang, Josep M. Guerrero, *Fellow Member*, *IEEE*, and Derek Abbott, *Fellow Member*, *IEEE*

***Abstract*—In this paper, a two-layer network and distributed control method is proposed, where there is a top layer communication network over a bottom layer microgrid. The communication network consists of two subgraphs, in which the first is composed of all agents, while the second is only composed of controllable agents. The distributed control laws derived from the first subgraph guarantee the supply-demand balance, while further control laws from the second subgraph reassign the outputs of controllable distributed generators, which ensure active and reactive power are dispatched optimally. However, for reducing the number of edges in the second subgraph, generally a simpler graph instead of a fully connected graph is adopted. In this case, a near-optimal dispatch of active and reactive power can be obtained gradually, only if controllable agents on the second subgraph calculate set points iteratively according to our proposition. Finally, the method is evaluated over seven cases via simulation. The results show that the system performs as desired, even if environmental conditions and load demand fluctuate significantly. In summary, the method can rapidly respond to fluctuations resulting in optimal power sharing.**

***Index Terms*—Distributed control, energy management, microgrids, multi-agent system (MAS), networked control systems, secondary control.**

I. Introduction

THE combustion of fossil fuels has caused a series of problems, such as smog, acid rain and environmental and economic concerns. Moreover, fossil fuel-fired electricity generation is the largest source of air pollution in many countries. Therefore, renewable energy electricity generation has drawn much attention all over the world [1]. However, the increasing penetration of renewable energy into a conventional grid also results in some negative impacts, such as the increasing fluctuations of voltages. Hence, in general, distributed generators (DGs) using renewable energies, energy storage systems and other equipment are integrated as a microgrid (MG) first, and then the MG is connected to a main grid, which is called a grid-connected mode [2], [3]. Certainly, an MG also can operate in an islanded mode, which has been applied in many remote areas and geographical islands. In this case, the control of an islanded MG is more difficult than that of a grid-connected MG, because the uncertainty of environmental conditions or inappropriate operation might cause voltage collapse without any support of the main grid [3].

In order to ensure MG stability, different control schemes for MGs have been proposed, such as hierarchical control [4]–[8], centralized control [9]–[11] and distributed or decentralized control [12]–[16]. In hierarchical control, there are several levels, which are primary control, secondary control, and sometimes tertiary control, where the primary control deals with DGs by local controllers (LCs) independently, while the secondary control maintains the electrical levels in the MG within the required values. Alternatively, in a centralized control scheme, all DGs are communicated with and managed by an MG central controller (MGCC), in which the failure of the MGCC is the most disturbing problem, because its failure may lead to complete loss of MG control. However, the DGs in decentralized control only contact with their local neighbors instead of the MGCC. As such, the complexity of communications can be reduced [7], and the failure of a single LC does not break the whole system down [5], [13], [17].

Therefore, distributed control has attracted much attention. Bidram *et al*. [14] proposed a multi objective control framework for an islanded MG, by which the voltage and frequency in the MG were synchronized to the nominal values, and the active and reactive power were dispatched in terms of power ratings of the inverters. In [18], the dispatch of the reactive power of the DGs in an MG was considered as a cooperative distributed optimization problem that was to minimize the sum of the voltage errors. Shafiee *et al*. [19] developed a distributed secondary control method based on a networked control system, and their experimental results have shown that the frequency and voltage steady-state errors were eliminated. A distributed control strategy for MGs with voltage source converters was proposed in [15], which was characterized by using instantaneous power theory. In [20], the authors presented a decentralized control scheme for islanded MGs, where a limited number of LCs had to be adjusted, if a DG

Manuscript received October 16, 2015; revised February 11, 2016 and April 6, 2016; accepted July 1, 2016. This work was supported by the National Natural Science Foundation of China under Grant No. 61105125 & No. 51177177, National "111" Project under Grant No. B08036 and Chongqing Basic and Frontier Research Project under Grant No. cstc2013jcyjA70006.

Q. Li, C. Peng, M. Chen, F. Chen and W. Kang are with the State Key Laboratory of Power Transmission Equipment & System Security and New Technology, School of Electrical Engineering, Chongqing University, Chongqing 400044, China (corresponding author Q. Li; phone: +862365112647; e-mail: qiangli.ac@gmail.com).

J. M. Guerrero is with the Department of Energy Technology, Aalborg University, 9220 Aalborg East, Denmark (e-mail: joz@et.aau.dk).

D. Abbott is with the School of Electrical and Electronic Engineering, University of Adelaide, SA 5005, Australia (e-mail: derek.abbott@adelaide.edu.au).

was plugged in or out. A distributed architecture for the control of islanded ac microgrids was also studied [21].

Recently, a multi-agent system (MAS) has been introduced for distributed control due to its complete distribution feature. For example, in a system composed of multi MGs, these MGs and power lines were considered as a team of cooperative agents in order to minimize the costs of energy storage among MGs, where convex optimization was used to solve the minimization problem [22]. Bidram *et al*. [23] described a distributed and adaptive voltage secondary control method with an agent-based communication network that was designed by using operations research techniques. In [24], distributed secondary voltage and frequency control methods were proposed, which consisted of two parts. If catastrophic disturbances occurred in MGs, an adaptive algorithm was developed to determine the local zones and the optimal strategies at zones first, and then a multi-agent control algorithm was used to maintain a stable voltage [25]. Also, a multi-agent system has been applied to the management of MGs with DGs and price-sensitive loads, in which DGs and loads were modeled as agents, and it was reported that the method was able to satisfy both the economic and the technical requirements of MGs [26].

In [27], Shafiee *et al*. proposed a cooperative control framework for an AC MG with a cyber network for data exchange, in which a dynamic consensus protocol was applied to regulate voltages and a reactive power regulator was designed to adjust the local droop coefficient dynamically. Their results showed that the global voltage regulation and proportional reactive power sharing were achieved. Also, inspired by cooperative control and average consensus algorithms, Simpson-Porco *et al*. [28] introduced distributed controllers for secondary frequency and voltage control in islanded MGs, which attained voltage regulation and reactive power sharing. Additionally, a consensus-based distributed voltage control method has been presented in [29], which guarantees reactive power sharing well, since the rigorous mathematical proof and analysis were provided.

As is known, some methods in the above mentioned papers are too complex to respond to the fluctuations of uncertain environmental conditions or/and load demand rapidly. Therefore, a simple and distributed method that responds to fluctuations rapidly and dispatches active and reactive power optimally is desired. Moreover, many studies have been performed for MGs where droop control is adopted. In contrast, there is little research in MGs where the active and reactive power control (PQ control) and voltage and frequency control (V/F control) are adopted. In this paper, a systematic control method is proposed for islanded MGs where DGs work in PQ or V/F control mode, which is a simple and completely distributed scheme. Furthermore, in the process of dispatch of power, the supply-demand balance is always satisfied and at the same time the fluctuations of the frequency and voltage in the system are minimal. In our method, the MG is considered as the bottom layer of a two layer model, while a communication network over the MG is considered as the top layer. Note that power flows in the MG that consists of DGs, while information spreads in the communication network that is composed of agents. The structure of the communication network is simple, so it is conveniently established by adding a few communication lines, when power line communication is adopted. Moreover, agents on the network can collect information from the DGs and loads to which they connect through the links between two layers, and then exchange these information with their neighbors on the communication network.

In this paper, there are four main technical contributions. First, in Section II, a systematic method is given, which consists of two parts. One is the rules to establish a communication network, and the other is the method to derive two sets of control laws based on the communication network. Second, two theorems are proved that ensure the power balance after adjustments through the secondary control, because it is desired that the outputs of the V/F DG return to zero gradually, after it injects or absorbs power into/from the system instantaneously, which is achieved by the secondary control. Third, optimal power dispatch can be obtained when the proposed control laws are applied. If the communication network is a fully connected network, after this control laws are used only once, the optimal power dispatch will be reached, as Theorem 3 states. On the other hand, if the network is not fully connected, the optimal power dispatch can be obtained by iterations, as shown in Proposition 1. Furthermore, the convergence rate is fast enough. Finally, a test bed is established in MATLAB/Simulink, which is a radial islanded MG. According to the results, it can be found that the system operates well, where the voltage and the frequency stay in a normal range, even if both environmental conditions and load demand fluctuate dramatically.

The rest of the paper is organized as follows. In Section II, at first, the structure of a communication network is given and the steps of how a communication network is established are described. Next, three theorems and a proposition are presented, which state how the control laws are obtained and how active and reactive power can be dispatched optimally. Section III introduces the structure of the MG and the parameters of DGs for simulations. Later, seven cases are designed to evaluate the performance of the control laws, in which some extreme situations are involved in Section IV, and then the simulation results are analyzed and discussed. Section V concludes the paper.

II. Control Method for MGs

This Section introduces some terms and the topology of a communication network first. Next, how the distributed control laws for agents are derived from the communication network is investigated, where three theorems and a proposition are presented.

A. Topology of Communication Network

In our method, a two layer model is employed, as shown in Fig. 1, where the top layer is a communication network for information transmission, while the bottom layer is the MG for power transmission. Generally speaking, most of DGs in an MG, such as photovoltaic (PV) systems or wind turbines (WTs), rely on renewable energies for power generation.

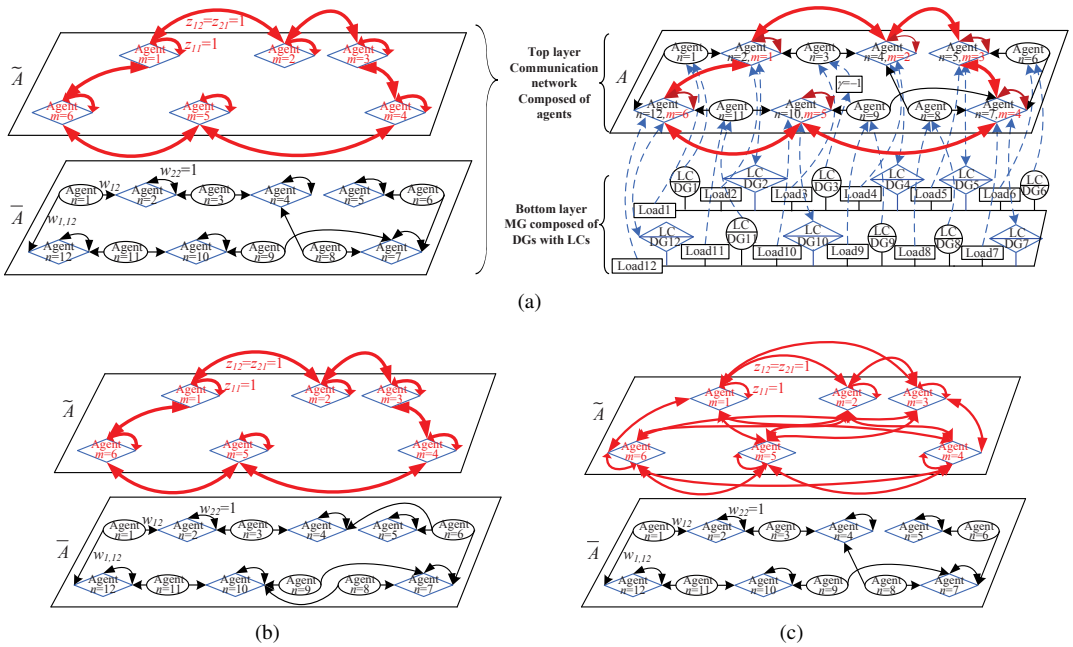

Fig. 1. The two-layer control model for an MG, where uncontrollable and partially controllable agents are indicated by circles, while controllable agents are indicated by diamonds. (a) Network 1. The left panel is the subgraph $\overline{A}$ composed of n agnets and the subgraph $\widetilde{A}$ composed of m controllable agents. The right panel is the communication network $A = G(V, E)$ and the MG. (b) Network 2. (c) Network 3.

However, environmental conditions always change over time, so the outputs of these DGs are uncertain. Therefore, these types of DGs are regarded as *uncontrollable* DGs. Conversely, there is another type of DGs, such as microturbines, which are considered as *controllable* DGs for their outputs can be controlled in terms of instructions. For an islanded MG, a battery energy storage system (BESS) working in a V/F control mode is generally needed, which provides the frequency and voltage references for the MG. Hence, it is regarded as a *partially controllable* DG.

On the other hand, there is a communication network $A = G(V, E)$ over the MG, which is a weighted and directed graph with n agents, where V is the set of agents (nodes) and E is the set of edges. In this paper, it is assumed that an agent is composed of communication devices together with a local control processor. Moreover, the agents who connect to uncontrollable DGs are referred as uncontrollable agents, while the agents who connect to controllable DGs and partially controllable DG are called controllable and partially controllable agents, respectively. The communication network in our model consists of two parts: i) the subgraph $\overline{A}$, in which the uncontrollable agents have outgoing edges but they do not have any ingoing edges, because uncontrollable agents never calculate and regulate the outputs of uncontrollable DGs to which they connect, while the controllable agents do not have any outgoing edges to uncontrollable agents, but have self loops. It is worth noting that the weight on an edge from an agent i to j is $w_{ij}, i \neq j$, while the weight on a self loop is always one, namely $w_{ii} = 1$; ii) the subgraph $\widetilde{A}$ with m nodes, is composed of only controllable agents, where each agent has both outgoing and ingoing edges. Note that self loops in $\overline{A}$ are shared in this subgraph, while the weights on all edges in $\widetilde{A}$ are always one. Therefore, this subgraph is a strongly connected and directed graph, since there exists a directed path from an agent i to an agent j and a directed path from j to i for every pair of agents i, j.

Moreover, each agent connects to a DG and a load through the links between two layers, where the arrows on the dashed lines (Fig. 1) indicate the direction of information transmission. Thus, it can not only acquire present states of a DG and a load to which it connects, but also send instructions to regulate the DG. Furthermore, agents also can exchange the information acquired with their neighbors on the communication network. Additionally, in our model, each agent basically handles a DG and a load, so the number of agents is equal to that of DGs and that of loads, which allows the sizes of matrices for the control laws to be equal. However, it is possible that the number of loads is greater than that of agents or DGs. In this case, a few loads nearby need to be regarded as a large load and then it is connected to an agent. On the contrary, if the number of loads is less than that of agents, some virtual loads with zero demand can be added to the MG in order to satisfy the requirement.

B. Distributed control laws

After a communication network is established, a set of control laws for agents should be derived from the network. Moreover, if the control laws are applied by agents to adjust the outputs of controllable DGs at each time, the system will be balanced and more importantly the outputs of controllable DGs are proportional to their maximal capacities, i.e., active and reactive power are optimally shared among controllable DGs. In this paper, we derive two sets of control laws from two subgraphs for controllable agents via the following two steps. First, the set points of controllable DGs at next time

step are calculated by controllable agents on $\overline{A}$ according to the first set of control laws, which balances the system. And then the agents on $\widetilde{A}$ recalculate the set points of controllable DGs according to the second set of control laws, which allows active and reactive power to be dispatched optimally.

As mentioned above, the communication network consists of two subgraphs. For the subgraph $\overline{A}$, it is a weighted and directed graph with n agents (nodes). An $n \times n$ matrix W is employed to describe the relations between nodes and indicate the weights on directed edges, in which if there is an edge from a node i to a node j, the entry is

$$w_{ij} = \frac{1}{u_i}, i \neq j, \tag{1}$$

where u_i is the number of outgoing edges of a node i. Otherwise, $w_{ij} = 0$. However, the weight on a self loop is $w_{ii} = 1$. Generally, the matrix W is not symmetrical, because there are not always two edges between every pair of nodes. But the sum of all elements in the ith row of W is always one,

$$\sum_{j=1}^{n} w_{ij} = 1. \tag{2}$$

Also, W^T represents the transpose of the matrix W. Further, we define an $n \times n$ and diagonal matrix B to indicate the type of an agent. In other words, when an agent i is a controllable agent, the corresponding entry b_{ii} is one. Otherwise, it is zero, when an agent is an uncontrollable agent or a partially controllable agent. Consecutively, a set of controllable agents can be defined as $\widetilde{V} = \{T(B \cdot V')\} \in V$, while the set of uncontrollable agents is $\overline{V} = V \backslash \widetilde{V}$. Here, $V \backslash \widetilde{V}$ means to obtain the complement of $\widetilde{V}$ in V and $V' = [v_i]_{n\times 1}$ is an $n \times 1$ column vector composed of n nodes, while $T(\cdot)$ is a function to return all nonzero elements in a vector.

Additionally, we deem the system is balanced, if the sum of outputs of controllable DGs at next time step $t+1$ is equal to the difference between the total amounts of load demand and the sum of outputs of uncontrollable DGs at time t,

$$\begin{cases} \sum [B \cdot P(t+1)] = \sum L^P(t) - \sum [(I-B) \cdot P(t)], \\ \sum [B \cdot Q(t+1)] = \sum L^Q(t) - \sum [(I-B) \cdot Q(t)], \end{cases} \tag{3}$$

where $P(t+1) = [P_i(t+1)]_{n\times 1}$, $Q(t+1) = [Q_i(t+1)]_{n\times 1}$, $L^P(t) = [L_i^P(t)]_{n\times 1}$ and $L^Q(t) = [L_i^Q(t)]_{n\times 1}$ are active power, reactive power, active load demand and reactive load demand column vectors, respectively, while I is an $n \times n$ identity matrix. As is known, there is a V/F DG in an islanded MG, which provides system losses in order to maintain the frequency and voltage constant in the system. In terms of the V/F control method, if there are errors between the frequency, voltage and their references, the V/F DG will inject or absorb power into/from the MG instantaneously in order to eliminate errors and then maintain the constant outputs. However, it is desired that the outputs of the V/F DG return to zero gradually, after it injects or absorbs power into/from the system instantaneously, which is achieved by the secondary control. Following this idea, a parameter $\gamma = -1$ is added between the V/F DG and its agent, before the agent sends this information to neighbors. In this way, the outputs of the V/F DG are considered as loads and then shared by controllable DGs. Consequently, based on the subgraph $\overline{A}$, the following control laws can be derived for controllable agents,

$$\begin{cases} B \cdot P(t+1) = B \cdot P(t) + W^T \cdot [L^P(t) - P(t)], \\ B \cdot Q(t+1) = B \cdot Q(t) + W^T \cdot [L^Q(t) - Q(t)], \end{cases} \tag{4}$$

and a theorem is determined.

Theorem 1: Let $\overline{A}$ be a weighted and directed subgraph with n agents, where agents are controllable, partially controllable or uncontrollable. Assume the kth agent is a partially controllable agent. If controllable agents calculate the set points of controllable DGs at next time step according to the control laws (4), then the system is balanced, namely, satisfying (3).

Proof: For (4), if both sides of the equation are summed up, respectively, we have

$$\begin{aligned} &\sum B \cdot P(t+1) = \sum B \cdot P(t) + \sum W^T \cdot \left[L^P(t) - P(t)\right] \\ &= (b_{11} \cdot P_1(t) + \cdots + b_{kk} \cdot \gamma \cdot P_k(t) + \cdots + b_{nn} \cdot P_n(t)) \\ &+ (w_{11} + w_{12} + \cdots + w_{1n}) \cdot [L_1^P(t) - P_1(t)] \\ &+ \cdots + (w_{k1} + w_{k2} + \cdots + w_{kn}) \cdot [L_k^P(t) - \gamma P_k(t)] \\ &+ \cdots + (w_{n1} + w_{n2} + \cdots + w_{nn}) \cdot [L_n^P(t) - P_n(t)]. \end{aligned} \tag{5}$$

According to (2), the above equation can be reexpressed as follows,

$$\begin{aligned} &\sum B \cdot P(t+1) = \sum B \cdot P(t) + \sum W^T \cdot \left[L^P(t) - P(t)\right] \\ &= (b_{11} \cdot P_1(t) + \cdots + b_{kk} \cdot \gamma \cdot P_k(t) + \cdots + b_{nn} \cdot P_n(t)) \\ &+ \left[L_1^P(t) - P_1(t)\right] + \cdots + \left[L_k^P(t) - \gamma \cdot P_k(t)\right] + \cdots \\ &+ \left[L_n^P(t) - P_n(t)\right] \\ &= ((b_{11} - 1) \cdot P_1(t) + \cdots + (b_{kk} - 1) \cdot \gamma \cdot P_k(t) + \cdots \\ &+ (b_{nn} - 1) \cdot P_n(t)) + \sum L^P(t) \\ &= \sum L^P(t) - \sum (I - B) \cdot P(t). \end{aligned} \tag{6}$$

Similarly, the other expression in (4) can be proved in exactly the same manner. ■

Apparently, if controllable agents apply (4) to adjust the outputs of controllable DGs, the system will be balanced. However, it is not always certain that active and reactive power are dispatched optimally among them, i.e., the outputs of controllable DGs are proportional to their capacities. Hence, the set points obtained in terms of (4) are recalculated based on the subgraph $\widetilde{A}$, before the controllable agents regulate the outputs of controllable DGs.

The subgraph $\widetilde{A}$ is composed of m controllable agents, so an $m \times m$ matrix $Z = [z_{ij}]_{m\times m}$ is used to represent the relations among controllable agents. The matrix Z is a symmetrical matrix, because it is a strongly connected and directed graph. Furthermore, the entries in the matrix are either ones or zeros, i.e., if there are two edges between each pair of nodes, then the two corresponding entries are ones. Otherwise, they are zeros. And the diagonal entries of the matrix Z are ones due to the shared self loops. Additionally, an $m \times m$ and diagonal degree matrix $D = [d_{ij}]_{m\times m}$ is also employed, where a degree of a node denotes the number of outgoing or ingoing edges of a node. The column vectors $\widetilde{C}_p = [\tilde{c}_i^p]_{m\times 1}$ is the maximal capacities, while $\widetilde{P} = [\tilde{p}_i]_{m\times 1}$ is set points of controllable

DGs that are calculated according to (4). Meanwhile, $\widetilde{P}$ also corresponds to the nonzero elements of the column vector $B \cdot P(t+1)$. According to the subgraph $\widetilde{A}$, we can derive the following control laws,

$$\begin{aligned} P'(t+1) &= [P'_i(t+1)]_{m\times 1} \\ &= \mathrm{diag}(\widetilde{C}_p) \cdot Z \cdot \left[\mathrm{diag}(Z \cdot \widetilde{C}_p)\right]^{-1} \cdot Z \cdot D^{-1} \cdot \widetilde{P} \\ &= \mathrm{diag}(\widetilde{C}_p) \cdot F \cdot \widetilde{P} = \mathrm{diag}(\widetilde{C}_p) \cdot H, \end{aligned} \tag{7}$$

where $P'(t+1)$ is the set points that controllable agents on $\widetilde{A}$ recalculate, $\mathrm{diag}(\cdot)$ denotes a function that creates a diagonal matrix from a corresponding vector and $[\cdot]^{-1}$ denotes the inverse of a matrix, while F is an $m \times m$ matrix and H is an $m \times 1$ column vector, $H = [h_i]_{m\times 1}$. In (7), information of neighbors of a controllable agent and that of their neighbors on $\widetilde{A}$ are involved, which is acquired by information exchange among neighbors for reducing the number of links. If "P" in (7) is replaced by "Q", the control laws for reactive power will be obtained. Consequently, it yields the theorem below.

Theorem 2: Let $\widetilde{A}$ be the subgraph with m controllable agents in the graph $A = G(V, E)$. If controllable agents on $\widetilde{A}$ recalculate set points of controllable DGs according to the control laws (7), then the system is still balanced, namely, satisfying $\sum P'(t+1) = \sum[B \cdot P(t+1)]$.

Proof: According to (7), the set point of the kth controllable DG can be recalculated as follows,

$$P'_k(t+1) = \sum_{i=1}^{m} \frac{z_{ki}\tilde{c}_k^p \left(\frac{z_{i1}\tilde{p}_1}{d_{11}} + \frac{z_{i2}\tilde{p}_2}{d_{22}} + \cdots + \frac{z_{im}\tilde{p}_m}{d_{mm}}\right)}{\sum_{j=1}^{m} z_{ij}\tilde{c}_j^p} = \tilde{c}_k^p \cdot h_k. \tag{8}$$

Therefore, the sum of outputs of all controllable DGs takes form

$$\begin{aligned} \sum_{k=1}^{m} P'_k(t+1) &= \sum_{k=1}^{m}\left[\sum_{i=1}^{m} \frac{z_{ki}\tilde{c}_k^p \left(\frac{z_{i1}\tilde{p}_1}{d_{11}} + \frac{z_{i2}\tilde{p}_2}{d_{22}} + \cdots + \frac{z_{im}\tilde{p}_m}{d_{mm}}\right)}{\sum_{j=1}^{m} z_{ij}\tilde{c}_j^p}\right] \\ &= \sum_{i=1}^{m}\left[\sum_{k=1}^{m} \frac{z_{ki}\tilde{c}_k^p \left(\frac{z_{i1}\tilde{p}_1}{d_{11}} + \frac{z_{i2}\tilde{p}_2}{d_{22}} + \cdots + \frac{z_{im}\tilde{p}_m}{d_{mm}}\right)}{\sum_{j=1}^{m} z_{ij}\tilde{c}_j^p}\right] \\ &= \sum_{i=1}^{m}\left(\frac{z_{i1}\tilde{p}_1}{d_{11}} + \frac{z_{i2}\tilde{p}_2}{d_{22}} + \cdots + \frac{z_{im}\tilde{p}_m}{d_{mm}}\right). \end{aligned} \tag{9}$$

Also, according to graph theory, the degree of a node is the sum of all elements in the jth column or the jth row of Z, so we have

$$d_{ii} = \sum_{i=1}^{m} z_{ij}. \tag{10}$$

Applying the above condition (10) to (9), the final result can be obtained as follows,

$$\begin{aligned} \sum_{k=1}^{m} P'_k(t+1) &= \tilde{p}_1 + \tilde{p}_2 + \cdots + \tilde{p}_m \\ &= \sum \widetilde{P} = \sum[B \cdot P(t+1)]. \ \blacksquare \end{aligned}$$

From the theorem 2, it can be found that the system is still balanced, after recalculating the set points of all controllable DGs in terms of the control laws (7). Furthermore, the control laws (7) also can make active and reactive power are shared optimally among controllable DGs, i.e., the outputs of controllable DGs are proportional to their capacities.

Theorem 3: If the subgraph $\widetilde{A}$ is a fully connected graph, then the outputs of controllable DGs are proportional to their capacities, i.e., $h_1 = h_2 = \cdots = h_m$, after the control laws (7) is applied to recalculate the set points of controllable DGs.

Proof: If the subgraph $\widetilde{A}$ is a fully connected graph, then the matrix Z is a matrix in which all entries are one, namely

$$z_{ij} = 1, \text{for all } i, j \in \{1, 2, \cdots, m\}. \tag{11}$$

Moreover, in this case, all degrees of nodes in the subgraph $\widetilde{A}$ are equal,

$$d_{11} = d_{22} = \cdots = d_{mm} = \sum_{i=1}^{m} z_{ki} = m. \tag{12}$$

If a controllable agent k recalculates the set point of the controllable DG to which it connects according to (7) or (8), then the coefficient h_k is

$$h_k = \sum_{i=1}^{m} \frac{z_{ki}\left(\frac{z_{i1}\tilde{p}_1}{d_{11}} + \frac{z_{i2}\tilde{p}_2}{d_{22}} + \cdots + \frac{z_{im}\tilde{p}_m}{d_{mm}}\right)}{\sum_{j=1}^{m} z_{ij}\tilde{c}_j^p}. \tag{13}$$

Applying the condition (11) and (12) to (13), we can obtain

$$h_k = \frac{\tilde{p}_1 + \tilde{p}_2 + \cdots + \tilde{p}_m}{\sum_{j=1}^{m} \tilde{c}_j^p} = \frac{\sum \widetilde{P}}{\sum \widetilde{C}_p}. \tag{14}$$

Therefore, according to (14), we have

$$h_1 = h_2 = \cdots = h_m,$$

so the outputs of controllable DGs are proportional to their capacities, i.e., active and reactive power are dispatched optimally. ■

In summary, there are two steps in finding the control laws that are used to calculate the set points of controllable DGs at next time. In the first step, a set of control laws (4) are obtained based on the subgraph $\widetilde{A}$, which guarantees the system to be balanced after the secondary control. However, it would be possible that not all outputs of controllable DGs were proportional to their capacities, if the control laws (4) were used to calculate the set points. Therefore, the second step is employed to slightly reassign the outputs among controllable DGs, which ensures active and reactive power are dispatched optimally. In other words, controllable agents on the subgraph $\widetilde{A}$ exchange the values of set points obtained from the first step, and then recalculate the set points of controllable DGs in terms of (7). After these two steps, controllable agents adjust the outputs of controllable DGs to which they connect according to the set points obtained at the second step.

On the other hand, if subgraph $\widetilde{A}$ is not a fully connected graph, then proportions of the outputs of controllable DGs to their capacities are not identical, after the second step is applied once. However, if the values of the set points of controllable DGs can be exchanged and calculated iteratively by controllable agents on the subgraph $\widetilde{A}$ for several times after the second step, then the proportions will approach each other. In other words, the set points of controllable DGs after k

iterations are $\text{diag}(\widetilde{C}_p)\cdot[\underbrace{F\cdot\text{diag}(\widetilde{C}_p)\cdot F\cdots\text{diag}(\widetilde{C}_p)\cdot F}_{k}]\cdot\widetilde{P}=\text{diag}(\widetilde{C}_p)\cdot Y\cdot\widetilde{P}$, which is shown by the following proposition.

Proposition 1: Assume there is a subgraph $\widetilde{A}$ with $m = 6$ nodes that is not a fully connected graph, as shown in Fig. 1, in which the degree of each node is $d = 3$, and the capacities of all controllable DGs are equal to $\tilde{c}_j^p = c \geq 10^4, j = 1,\cdots,m$. After $k = 3$ iterations in terms of (7), the absolute value of the difference between each entry in Y and $1/\sum_{j=1}^m \tilde{c}_j^p$ is less than 0.03×10^{-4}. Therefore, the proportions of the outputs of controllable DGs to their capacities are approximately equal to $\sum\widetilde{P}/\sum\widetilde{C}_p$.

Proof: According to (7), the outputs of controllable DGs after three iterations are

$$\text{diag}(\widetilde{C}_p)\cdot[F\cdot\text{diag}(\widetilde{C}_p)\cdot F\cdot\text{diag}(\widetilde{C}_p)\cdot F]\cdot\widetilde{P}=\text{diag}(\widetilde{C}_p)\cdot Y\cdot\widetilde{P}. \quad (15)$$

Next, if the absolute value of difference between $1/\sum_{j=1}^m \tilde{c}_i^p$ and each entry in Y is calculated, we can obtain the following matrix,

$$\left|\frac{1}{\sum_{i=1}^m \tilde{c}_i^p}\cdot\mathbf{1}_{m\times m}-Y\right| = \frac{1}{4374c}\begin{bmatrix}129&63&63&129&63&63\\63&129&63&63&129&63\\63&63&129&63&63&129\\129&63&63&129&63&63\\63&129&63&63&129&63\\63&63&129&63&63&129\end{bmatrix}, \quad (16)$$

where $\mathbf{1}_{m\times m}$ is an $m\times m$ matrix whose all entries are 1. Apparently, the maximal difference is less than or equal to $129/4374c = 0.03\times10^{-4}$ due to $c \geq 10^4$, which means all entries in Y are approximately equal to $1/\sum_{j=1}^m \tilde{c}_i^p$. Therefore, the final proportions $H = Y\cdot\widetilde{P}$ of the outputs of controllable DGs to their capacities are approximately equal, namely $h_1 \approx h_2 \approx \cdots \approx h_m \approx \sum\widetilde{P}/\sum\widetilde{C}_p$. ■

In fact, as m increases, the Proposition 1 still holds. Furthermore, the structure of the subgraph $\widetilde{A}$ is the structure with the least edges and at the same time keeps the subgraph $\widetilde{A}$ connected without isolated nodes. If other structure that is not a fully connected graph is adopted, the degrees of nodes on $\widetilde{A}$ need to be identical.

III. Microgrid System Architecture

A test bed is established in MATLAB/Simulink in order to evaluate the performance of our method, which is a radial islanded MG that consists of 12 DGs and 12 loads. Moreover, a communication network composed of agents is also developed based on the blocks, called MATLAB Function, in MATLAB/Simulink. In 12 DGs of the MG, there are six controllable DGs, and five uncontrollable DGs and a partially controllable DG. The six controllable DGs are considered as ideal DC voltage sources V_{dc} [30]–[32] that work in the PQ control mode, while the five uncontrollable DGs are PVs and permanent magnet synchronous generator wind turbines (PMSG-WTs), which all work in the maximum power point tracking (MPPT) control mode. Furthermore, the partially controllable DG is implemented by a BESS, which can inject or/and absorb power into/from the MG in order to maintain the voltage and the frequency constant. When the MG is established in MATLAB/Simulink, physical constraints of these DGs are also considered. For example, the outputs of each DG cannot exceed its maximal capacity and the outputs of controllable DGs cannot be less than zero, even if the set points are less than zero. Moreover, the instantaneous output of the BESS is limited and there is a capacity constraint, when the BESS charges or discharges.

Finally, all parameters of these DGs and loads are listed in Table I. It is worth noting that the large loads are arranged near the DGs with small capacities, while the small loads near the DGs with large capacities. In this case, it is more difficult to satisfy the supply-demand balance and the optimal power dispatch in the MG by the distributed control laws. Throughout simulations, it is assumed that all uncontrollable DGs do not produce any reactive power, because the control of the active and reactive power of WTs and PVs is decoupled, while the line voltage and the frequency in the MG are set at 380 V and 50 Hz, respectively. Furthermore, the line losses in the MG are considered, since the line impedance is set at $0.169 + j0.07$ Ω/km. Note that the MG system works in a balanced state initially.

TABLE I
Setup and Parameters of DGs and Loads

Sources	Capacities	Control	Load	Max. Demand
DG_1	50 kW, 0 kVar	MPPT	$Load_1$	40 kW, 0 kVar
DG_2	40 kW, 20 kVar	PQ	$Load_2$	35 kW, 15 kVar
DG_3	**30 Ah**	**V/F**	$Load_3$	15 kW, 0 kVar
DG_4	60 kW, 30 kVar	PQ	$Load_4$	10 kW, 10 kVar
DG_5	40 kW, 20 kVar	PQ	$Load_5$	30 kW, 0 kVar
DG_6	30 kW, 0 kVar	MPPT	$Load_6$	35 kW, 15 kVar
DG_7	60 kW, 30 kVar	PQ	$Load_7$	15 kW, 10 kVar
DG_8	30 kW, 0 kVar	MPPT	$Load_8$	30 kW, 15 kVar
DG_9	50 kW, 0 kVar	MPPT	$Load_9$	15 kW, 0 kVar
DG_{10}	40 kW, 20 kVar	PQ	$Load_{10}$	25 kW, 0 kVar
DG_{11}	30 kW, 0 kVar	MPPT	$Load_{11}$	30 kW, 15 kVar
DG_{12}	60 kW, 30 kVar	PQ	$Load_{12}$	10 kW, 10 kVar

Further, on the subgraph $\overline{A}$, uncontrollable agents send their information to controllable agents once in every 10 ms, and then controllable agents calculate the set points of controllable DGs in terms of (4). Thereafter, this information is exchanged by controllable agents on $\widetilde{A}$ and the set points of controllable DGs are recalculated according to (7). On the other hand, note that in the period of time when information is not transmitted on the subgraph $\overline{A}$, controllable agents on the subgraph $\widetilde{A}$ send the current values of set points of controllable DGs to their neighbors at every 1 ms. Further, the set points of controllable DGs are recalculated iteratively according to (7) and then the outputs of controllable DGs are regulated. In this way, active and reactive power are dispatched approximately optimally among controllable DGs gradually, even if the communication network is not a fully connected network, as the proposition 1 states.

IV. Results

To evaluate the performance of our method, seven cases are designed, in which the relationship between the changes of

environmental conditions and the performance is studied first, and then the fluctuations of load demand are considered, and also how both the environmental conditions and load demand influence the performance at the same time is investigated. Later, our method is tested, when different topologies of communication networks are applied. Further, time delays, package losses and link failures are considered, respectively. Finally, all results are shown and discussed.

A. Case 1: Environmental conditions fluctuations

In the MG, there are two PVs and three WTs, whose outputs rely on environmental conditions. In this case, the outputs of uncontrollable DGs are designed and shown in Fig. 2(a). Simulations are performed to study the impact of environmental conditions on the system, when the network $A = G(V, E)$ in Fig. 1(a) is employed as the communication network and the control laws (4) and (7) are applied. According to Theorem 1, the first set of control laws (4) is as follows,

$$\begin{aligned}
P_2(t+1) &= \frac{1}{2}L_1^P(t) + L_2^P(t) + \frac{1}{2}L_3^P(t) - \frac{1}{2}P_1(t) - \frac{1}{2}\gamma \cdot P_3(t)\\
P_4(t+1) &= \frac{1}{2}L_3^P(t) + L_4^P(t) + \frac{1}{2}L_8^P(t) - \frac{1}{2}\gamma \cdot P_3(t) - \frac{1}{2}P_8(t)\\
P_5(t+1) &= L_5^P(t) + \frac{1}{2}L_6^P(t) - \frac{1}{2}P_6(t)\\
P_7(t+1) &= \frac{1}{2}L_6^P(t) + L_7^P(t) + \frac{1}{2}L_8^P(t) + \frac{1}{2}L_9^P(t)\\
&\quad - \frac{1}{2}P_6(t) - \frac{1}{2}P_8(t) - \frac{1}{2}P_9(t)\\
P_{10}(t+1) &= \frac{1}{2}L_9^P(t) + L_{10}^P(t) + \frac{1}{2}L_{11}^P(t) - \frac{1}{2}P_9(t) - \frac{1}{2}P_{11}(t)\\
P_{12}(t+1) &= \frac{1}{2}L_1^P(t) + \frac{1}{2}L_{11}^P(t) + L_{12}^P(t) - \frac{1}{2}P_1(t) - \frac{1}{2}P_{11}(t).
\end{aligned}$$

Before Theorem 2 is applied, the following matrices need to be written first,

$$Z = \begin{bmatrix} 1 & 1 & 0 & 0 & 0 & 1\\ 1 & 1 & 1 & 0 & 0 & 0\\ 0 & 1 & 1 & 1 & 0 & 0\\ 0 & 0 & 1 & 1 & 1 & 0\\ 0 & 0 & 0 & 1 & 1 & 1\\ 1 & 0 & 0 & 0 & 1 & 1 \end{bmatrix}, D = \begin{bmatrix} 3 & 0 & 0 & 0 & 0 & 0\\ 0 & 3 & 0 & 0 & 0 & 0\\ 0 & 0 & 3 & 0 & 0 & 0\\ 0 & 0 & 0 & 3 & 0 & 0\\ 0 & 0 & 0 & 0 & 3 & 0\\ 0 & 0 & 0 & 0 & 0 & 3 \end{bmatrix}. \quad (17)$$

Thus, the second set of control laws (7) can be written in terms of (8) one by one.

The results are shown in Fig. 2(b) and (c), where Fig. 2(b) is the outputs of controllable DGs, while Fig. 2(c) is the frequency of the system and the line voltages at the head and the tail of the bus, which are represented by the voltages of Load2 and Load12, respectively. From Fig. 2, it can be seen that the system operates well, because the voltage and the frequency remain constant, and they always stay at 380 V and 50 Hz respectively throughout simulations. Moreover, the outputs of all controllable DGs remain smooth and they are proportional to their capacities, which means the control laws can adjust controllable DGs accurately to follow the fluctuations of environmental conditions. Therefore, the outputs of the V/F DG are always zero, i.e., it does not need to inject or absorb any power into/from the system.

B. Case 2: Load demand fluctuations

As is known, if load demand fluctuates significantly, the voltage and the frequency in the system will be influenced negatively. But it offers an effective way to test the performance of the control laws. Hence, during simulations, the load demand is scheduled as below,

- $t = 2$ s: all active and reactive power loads increase by 20%,
- $t = 4$ s: Load_1 and Load_6 are cut from the MG,
- $t = 6$ s: all active and reactive power loads decrease by 20%,
- $t = 8$ s: Load_1 and Load_6 are connected to the MG,

while the outputs of all uncontrollable DGs are always at 40% of their capacities.

Under this settings, simulations are carried out on Network 1 and the results are shown in Fig. 3. Unlike the smooth voltage and frequency in Fig. 2, in this case, the voltage and frequency fluctuate significantly at some instances, but the fluctuations are short-lived, when load demand changes dramatically. However, the voltage and frequency at other times are smooth. Additionally, the fluctuations of outputs of the V/F DG are similar to those of voltages, but it can be seen that the outputs of the V/F DG return to zero, after it injects or absorbs power instantaneously, because its outputs are shared by controllable DGs.

In simulations, agents corresponding to uncontrollable and partially controllable DGs always send their information to the agents of controllable DGs. Thereafter, controllable agents calculate the set points of controllable DGs according to these information, and then they send the values to other controllable agents, as shown in the subgraph $\widetilde{A}$. Finally, controllable agents recalculate the set points after receiving these values and regulate the outputs of controllable DGs at next time. Therefore, the outputs of all controllable DGs, active and reactive power, are dispatched very well, as shown in Fig. 3(b).

C. Case 3: Both environmental conditions and load demand fluctuations

In previous two sections, when either environmental conditions or load demand changes over time, the control laws can respond rapidly to the fluctuations in the system and keep the system stable. However, in this section, the performance of the control laws is investigated, when both environmental conditions and load demand fluctuate at the same time, which is a severe test for the control laws. In this case, the settings for environmental conditions follow those in Case 1, while the settings for load demand take those in Case 2. Simulations are carried out on Network 1 under these settings and the results are shown in Fig. 4.

From the results, it can be found that the system runs well, where the voltages and the frequency in Fig. 4(c) vary slightly, except the extremely situations when the load demand fluctuates dramatically. But, even in these situations, the voltages and the frequency still keep in a normal range. Furthermore, the outputs of all controllable DGs are approximately proportional to their capacities according to the proposition 1, since the subgraph $\widetilde{A}$ in Fig. 1 is not a fully connected graph.

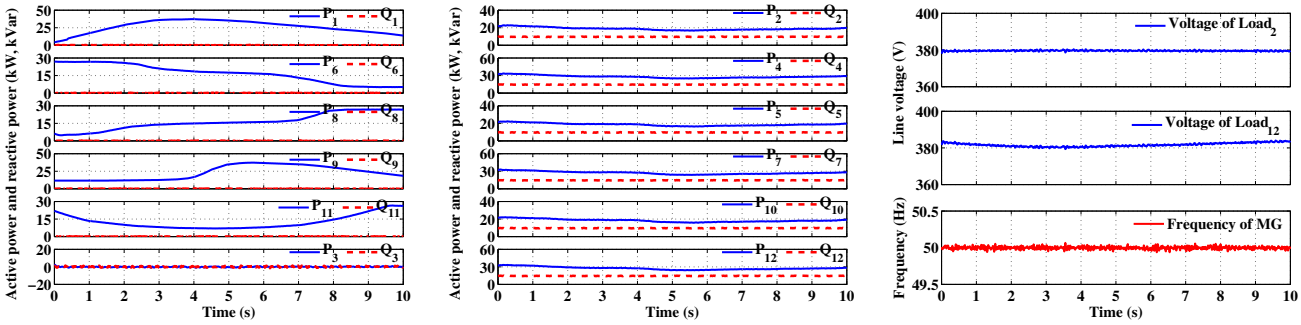

Fig. 2. Simulation results when only environmental conditions change over time. (a) Active and reactive power outputs of uncontrollable and partially controllable. (b) Active and reactive power outputs of controllable DGs. (c) The line voltages and frequency in the MG.

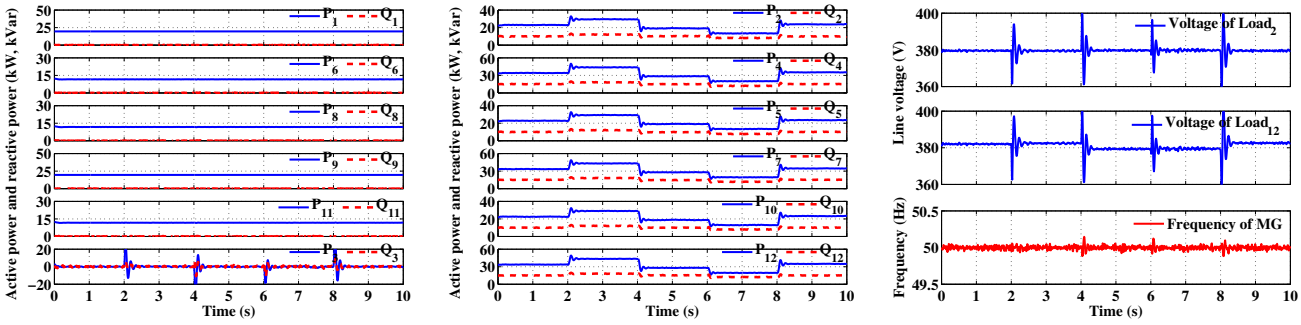

Fig. 3. Simulation results when load demand changes over time. (a) Active and reactive power outputs of uncontrollable and partially controllable. (b) Active and reactive power outputs of controllable DGs. (c) The line voltages and frequency in the MG.

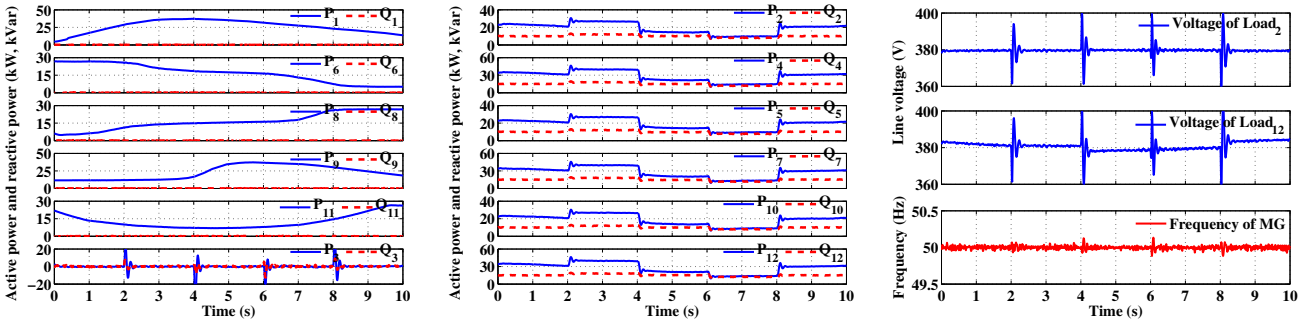

Fig. 4. Simulation results when both environmental conditions and load demand fluctuate over time. (a) Active and reactive power outputs of uncontrollable and partially controllable. (b) Active and reactive power outputs of controllable DGs. (c) The line voltages and frequency in the MG.

If a fully connected subgraph is applied, those outputs are completely proportional to their capacities. On the other hand, there are 30 edges in a fully connected subgraph, in contrast to six edges in the currently used subgraph $\widetilde{A}$. Moreover, if the power line communication is employed, the edges that need to be added are much less than those in a fully connected subgraph.

Additionally, as shown in Fig. 4(a), the outputs of the V/F DG return to zero, after immediate power injection or absorption, which is consistent with our expectation. This is because controllable DGs share the outputs of the V/F DG that are considered as loads in terms of the method mentioned in Section II. In summary, the control laws can handle the situations very well, when both environmental conditions and load demand fluctuate over time. Even if there are some extreme variations in the system, the system still remains stable.

D. Case 4: The topologies of communication networks vs. the performance of the system

As shown in Fig. 1(b) and (c), two different communication networks are designed to evaluate the relationship between the topologies of networks and the performance of the system. Compared with the original network in Fig. 1(a), Network 2

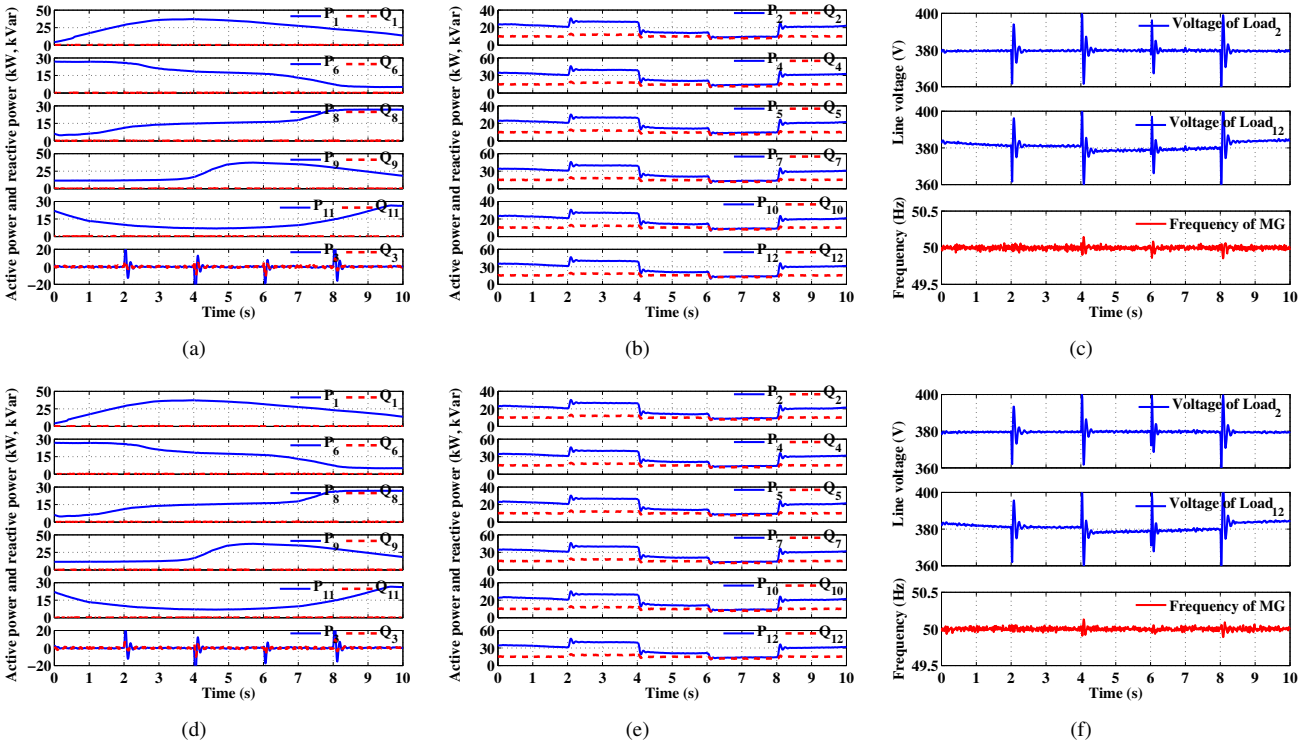

Fig. 5. Simulation results under different topologies, when both environmental conditions and load demand fluctuate over time. (a),(d) Active and reactive power outputs of uncontrollable and partially controllable. (b),(e) Active and reactive power outputs of controllable DGs. (c),(f) The line voltages and frequency in the MG. (a)-(c) on Network 2. (d)-(f) on Network 3.

is added more edges on the subgraph $\overline{A}$, while the subgraph $\widetilde{A}$ remains the same. On the other hand, in Network 3, the subgraph $\overline{A}$ does not change, while the subgraph $\widetilde{A}$ is replaced by a fully connected network. Here, all settings follow those in Case 3.

The simulation results obtained on two networks are shown in Fig. 5, when both environmental conditions and load demand fluctuate over time. From the results, it can be found that the outputs of controllable DGs and voltages and frequency are almost the same when different communication networks are adopted, which means our method is not associated with topologies of networks strongly. Therefore, it is more convenient to design a communication network without many restrictions.

E. Case 5: Impacts of time delays when both environmental conditions and load demand fluctuate

In a real communication network, sometimes time delays are unavoidable when information is transmitted on the network. For our method, the communication network over the MG plays an important role in order to ensure the system performs well. Therefore, in this section, how time delays influence the performance of the MG is studied, when both environmental conditions and load demand fluctuate over time, where the settings follow those in Case 3. Moreover, a fixed time delay α occurs, which is implemented by a block called Variable Integer Delay in MATLAB/Simulink, once information is transmitted from one agent to another at each time step.

In order to test the control laws, different time delays, $\alpha = 10, 20, 30$ ms, are applied in the system. For sake of simplicity, only voltages and frequency in simulation results are shown in Fig. 6. Compared with the results without time delays, the fluctuations of voltages and frequency last longer, after a large change occurs. But eventually voltages and frequency return to prescribed values gradually and they always stay in a normal range. Further, from Fig. 6, it can be noticed that the longer the time delays are, the longer the fluctuations last. This is because agents at time t always deal with the information acquired at time $t-\alpha$. In this case, it is difficult for agents to take effective actions to respond to the changes in the system immediately.

F. Case 6: Impacts of package losses when both environmental conditions and load demand fluctuate

When a communication network does not work stably, e.g. network congestion occurs, package losses may occur. In this section, the influence of package losses on performance is investigated, when both environmental conditions and load demand fluctuate over time, where the settings follow those in Case 3. Here, it is assumed that the probability of package losses on the subgraph $\widetilde{A}$ is 0.5, when information transmits on the communication network. According to the statistical results in Fig. 7, it is seen that the fluctuations of outputs of controllable DGs increase significantly, but its large-scale behavior is still similar to that without any package losses. Meanwhile, voltages and frequency in the system vary more, but they still stay in a normal range.

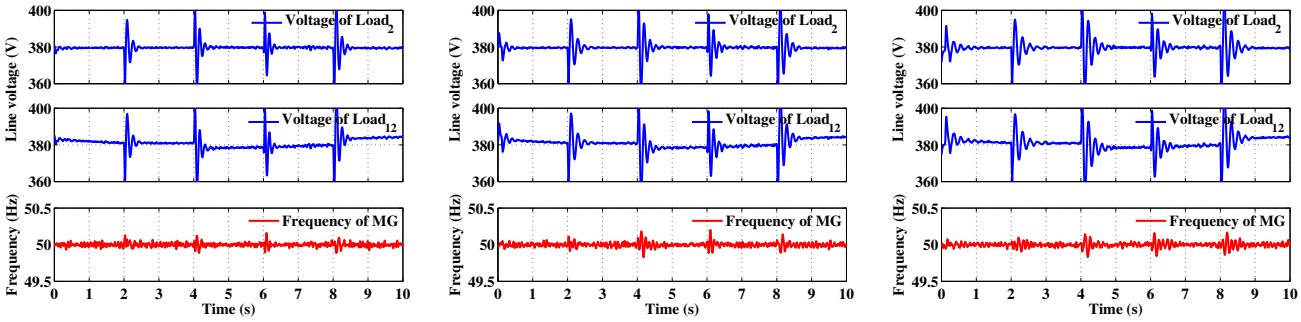

Fig. 6. Simulation results under different time delays, when both environmental conditions and load demand fluctuate over time. (a) α = 10 ms, (b) α = 20 ms, (c) α = 30 ms.

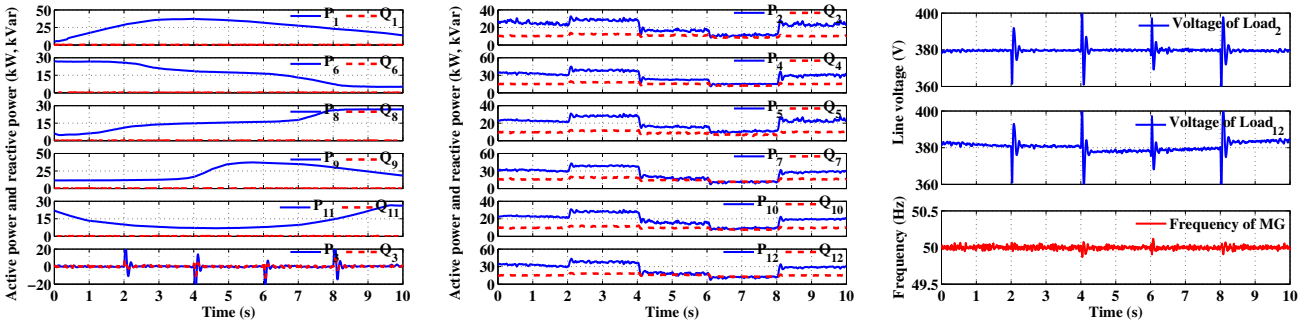

Fig. 7. Simulation results under package losses, when both environmental conditions and load demand fluctuate over time. (a) Active and reactive power outputs of uncontrollable and partially controllable. (b) Active and reactive power outputs of controllable DGs. (c) The line voltages and frequency in the MG.

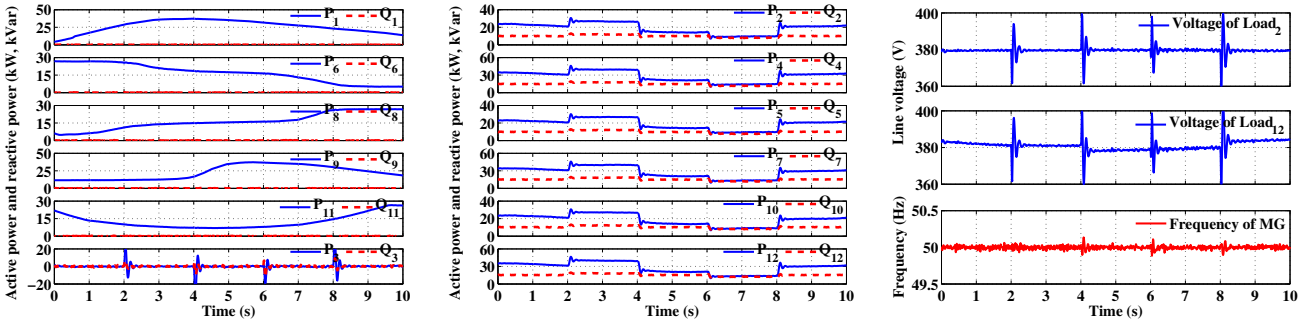

Fig. 8. Simulation results if link failures occur, when both environmental conditions and load demand fluctuate over time. (a) Active and reactive power outputs of uncontrollable and partially controllable. (b) Active and reactive power outputs of controllable DGs. (c) The line voltages and frequency in the MG.

G. Case 7: Link failures vs. the performance of the system

As mentioned in the previous section, the change of topologies of networks does not affect the performance of the system significantly. However, it is important to clarify how link failures influence the performance of the system if they occur, when the system is running. Therefore, we investigate the impact of link failures on the performance, when the links e_{64} and $e_{8,10}$ on the subgraph $\overline{A}$ are broken at t = 3 and then are restored at t = 7, while the other settings follow those in Case 3. As shown in Fig. 8, we can see that the system still works well, even if two links fail. On the other hand, it should be emphasized that isolated agents on the network are not allowed, and for such extreme failure the system will malfunction.

V. Conclusion

We have proposed a networked and distributed control model for islanded MGs, which consists of two layers, i.e., the bottom layer is the MG, while the top layer is the communication network composed of agents. The communication network

is a key component of our method, which is composed of two subgraphs $\overline{A}$ and $\widetilde{A}$, where the controllable agents and their self-loops are shared by these two subgraphs. Correspondingly, the set points of controllable DGs at next time are obtained by two steps. At first, uncontrollable agents on the subgraph $\overline{A}$ send their collected information to controllable agents. When they receive this information, they calculate the set points of controllable DGs in terms of the control laws (4). Thereafter, controllable agents on the subgraph $\widetilde{A}$ exchange these values with their neighbors. And then the latest set points of controllable DGs are recalculated by controllable agents according to the control laws (7). Consequently, they are applied to regulate the outputs of controllable DGs at next time by the controllable agents.

In our model, the communication network plays an important role, so the method of how to construct the two subgraphs is given first. Once the network is established, one can obtained the control laws in terms of Theorem 1 and 2, which guarantee that the system are balanced after the secondary control, only if the control laws are employed by agents to adjust the outputs of controllable DGs. On the other hand, these two theorems do not provide any information about if active and reactive power are dispatched optimally, i.e., the outputs of controllable DGs are proportional to their capacities. Therefore, Theorem 3 is proved, which states that the outputs of controllable DGs are completely proportional to their capacities after the control laws (7) are applied once, if the subgraph $\widetilde{A}$ is a fully connected graph.

In order to evaluate the performance of the control laws, seven cases are designed, where in the first two cases, either environmental conditions or load demand fluctuates, while in the last five cases, both environmental conditions and load demand change at the same time. From the simulation results that we obtained, the system always operates well. In other words, the voltages and the frequency stay close to the prescribed values, and are always kept in a normal range, even if environmental conditions and load demand vary dramatically. Furthermore, active and reactive power are shared approximately optimally by controllable DGs in terms of the proposition 1, even if the subgraph $\widetilde{A}$ is not a fully connected graph, due to reducing the number of edges in the subgraph. In summary, our method can not only respond to those changes of environmental conditions and load demand rapidly, but also allows active and reactive power to be dispatched approximately optimally. For future work, considering a distributed control method with optimal dispatch in a competitive environment is a significant question.

REFERENCES

[1] D. Abbott, "Keeping the energy debate clean: How do we supply the world's energy needs?" *Proc. IEEE*, vol. 98, no. 1, pp. 42–66, Jan. 2010.

[2] R. H. Lasseter and P. Paigi, "Microgrid: a conceptual solution," in *IEEE 35th Annual Power Electronics Specialists Conference*, vol. 6, Jun. 2004, pp. 4285–4290.

[3] R. Lasseter, "Smart distribution: Coupled microgrids," *Proc. IEEE*, vol. 99, no. 6, pp. 1074–1082, Jun. 2011.

[4] J. M. Guerrero, J. C. Vasquez, J. Matas, L. G. de Vicuña, and M. Castilla, "Hierarchical control of droop-controlled ac and dc microgrids - a general approach toward standardization," *IEEE Trans. Ind. Electron.*, vol. 58, no. 1, pp. 158–172, Jan. 2011.

[5] J. M. Guerrero, M. Chandorkar, T. L. Lee, and P. C. Loh, "Advanced control architectures for intelligent microgrids—Part I: Decentralized and hierarchical control," *IEEE Trans. Ind. Electron.*, vol. 60, no. 4, pp. 1254–1262, Apr. 2013.

[6] J. Vasquez, J. Guerrero, M. Savaghebi, J. Eloy-Garcia, and R. Teodorescu, "Modeling, analysis, and design of stationary-reference-frame droop-controlled parallel three-phase voltage source inverters," *IEEE Trans. Ind. Electron.*, vol. 60, no. 4, pp. 1271–1280, Apr. 2013.

[7] M. Yazdanian and A. Mehrizi-Sani, "Distributed control techniques in microgrids," *IEEE Trans. Smart Grid*, vol. 5, no. 6, pp. 2901–2909, Nov. 2014.

[8] Q. Shafiee, C. Stefanovic, T. Dragicevic, P. Popovski, J. Vasquez, and J. Guerrero, "Robust networked control scheme for distributed secondary control of islanded microgrids," *IEEE Trans. Ind. Electron.*, vol. 61, no. 10, pp. 5363–5374, Oct. 2014.

[9] K. T. Tan, X. Y. Peng, P. L. So, Y. C. Chu, and M. Z. Q. Chen, "Centralized control for parallel operation of distributed generation inverters in microgrids," *IEEE Trans. Smart Grid*, vol. 3, no. 4, pp. 1977–1987, Dec. 2012.

[10] M. M. A. Abdelaziz, M. F. Shaaban, H. E. Farag, and E. F. El-Saadany, "A multistage centralized control scheme for islanded microgrids with pevs," *IEEE Trans. Sustain. Energy*, vol. 5, no. 3, pp. 927–937, Jul. 2014.

[11] D. Olivares, C. Cañizares, and M. Kazerani, "A centralized energy management system for isolated microgrids," *IEEE Trans. Smart Grid*, vol. 5, no. 4, pp. 1864–1875, Jul. 2014.

[12] H. Kumar Nunna and S. Doolla, "Multiagent-based distributed-energy-resource management for intelligent microgrids," *IEEE Trans. Ind. Electron.*, vol. 60, no. 4, pp. 1678–1687, Apr. 2013.

[13] D. Olivares, A. Mehrizi-Sani, A. Etemadi, C. Canizares, R. Iravani, M. Kazerani, A. Hajimiragha, O. Gomis-Bellmunt, M. Saeedifard, R. Palma-Behnke, G. Jimenez-Estevez, and N. Hatziargyriou, "Trends in microgrid control," *IEEE Trans. Smart Grid*, vol. 5, no. 4, pp. 1905–1919, Jul. 2014.

[14] A. Bidram, A. Davoudi, and F. Lewis, "A multiobjective distributed control framework for islanded ac microgrids," *IEEE Trans. Ind. Informat.*, vol. 10, no. 3, pp. 1785–1798, Aug. 2014.

[15] A. Ovalle, G. Ramos, S. Bacha, A. Hably, and A. Rumeau, "Decentralized control of voltage source converters in microgrids based on the application of instantaneous power theory," *IEEE Trans. Ind. Electron.*, vol. 62, no. 2, pp. 1152–1162, Feb. 2015.

[16] Y. Xu and Z. Li, "Distributed optimal resource management based on the consensus algorithm in a microgrid," *IEEE Trans. Ind. Electron.*, vol. 62, no. 4, pp. 2584–2592, Apr. 2015.

[17] A. G. Tsikalakis and N. D. Hatziargyriou, "Centralized control for optimizing microgrids operation," *IEEE Trans. Energy Convers.*, vol. 23, no. 1, pp. 241–248, Mar. 2008.

[18] A. Maknouninejad and Z. Qu, "Realizing unified microgrid voltage profile and loss minimization: A cooperative distributed optimization and control approach," *IEEE Trans. Smart Grid*, vol. 5, no. 4, pp. 1621–1630, Jul. 2014.

[19] Q. Shafiee, J. Guerrero, and J. Vasquez, "Distributed secondary control for islanded microgrids-a novel approach," *IEEE Trans. Power Electron.*, vol. 29, no. 2, pp. 1018–1031, Feb. 2014.

[20] S. Riverso, F. Sarzo, and G. Ferrari-Trecate, "Plug-and-play voltage and frequency control of islanded microgrids with meshed topology," *IEEE Trans. Smart Grid*, vol. 6, no. 3, pp. 1176–1184, May. 2015.

[21] S. Cady, A. Dominguez-Garcia, and C. Hadjicostis, "A distributed generation control architecture for islanded ac microgrids," *IEEE Trans. Control Syst. Technol.*, vol. 23, no. 5, pp. 1717–1735, Sep. 2015.

[22] H. Dagdougui and R. Sacile, "Decentralized control of the power flows in a network of smart microgrids modeled as a team of cooperative agents," *IEEE Trans. Control Syst. Technol.*, vol. 22, no. 2, pp. 510–519, Mar. 2014.

[23] A. Bidram, F. L. Lewis, and A. Davoudi, "Distributed control systems for small-scale power networks: Using multiagent cooperative control theory," *IEEE Control Systems*, vol. 34, no. 6, pp. 56–77, Dec. 2014.

[24] F. Guo, C. Wen, J. Mao, and Y.-D. Song, "Distributed secondary voltage and frequency restoration control of droop-controlled inverter-based microgrids," *IEEE Trans. Ind. Electron.*, vol. 62, no. 7, pp. 4355–4364, Jul. 2015.

[25] S. Islam, K. Muttaqi, and D. Sutanto, "A decentralized multiagent-based voltage control for catastrophic disturbances in a power system," *IEEE Trans. Ind. Appl.*, vol. 51, no. 2, pp. 1201–1214, Mar. 2015.

[26] Y. Foo Eddy, H. Gooi, and S. Chen, "Multi-agent system for distributed management of microgrids," *IEEE Trans. Power Syst.*, vol. 30, no. 1, pp. 24–34, Jan. 2015.

[27] Q. Shafiee, V. Nasirian, J. M. Guerrero, F. L. Lewis, and A. Davoudi, "Team-oriented adaptive droop control for autonomous ac microgrids," in *Proc. IEEE 40th Annu. Ind. Electron. Soc. Conf.*, Oct. 2014, pp. 1861–1867.
[28] J. Simpson-Porco, Q. Shafiee, F. Dorfler, J. Vasquez, J. Guerrero, and F. Bullo, "Secondary frequency and voltage control of islanded microgrids via distributed averaging," *IEEE Trans. Ind. Electron.*, vol. 62, no. 11, pp. 7025–7038, Nov. 2015.
[29] J. Schiffer, T. Seel, J. Raisch, and T. Sezi, "Voltage stability and reactive power sharing in inverter-based microgrids with consensus-based distributed voltage control," *IEEE Trans. Control Syst. Technol.*, vol. 24, no. 1, pp. 96–109, Jan. 2016.
[30] N. Pogaku, M. Prodanovic, and T. Green, "Modeling, analysis and testing of autonomous operation of an inverter-based microgrid," *IEEE Trans. Power Electron.*, vol. 22, no. 2, pp. 613–625, Mar. 2007.
[31] R. Majumder, A. Ghosh, G. Ledwich, and F. Zare, "Power management and power flow control with back-to-back converters in a utility connected microgrid," *IEEE Trans. Power Syst.*, vol. 25, no. 2, pp. 821–834, May. 2010.
[32] R. Majumder, B. Chaudhuri, A. Ghosh, R. Majumder, G. Ledwich, and F. Zare, "Improvement of stability and load sharing in an autonomous microgrid using supplementary droop control loop," *IEEE Trans. Power Syst.*, vol. 25, no. 2, pp. 796–808, May. 2010.

Qiang Li received the B.S. degree in electrical engineering from the Sichuan Institute of Technology, Chengdu, China, in 2001; the M.S. degree in control theory and engineering from Chongqing University, Chongqing, China, in 2004; and the Ph.D. degree in electrical engineering from Zhejiang University, Hangzhou, China, in 2009. He was a Post-Doctoral Fellow with Chongqing University from 2009 to 2012 and a Visiting Post-Doctoral Scholar with the University of Adelaide, Adelaide, SA, Australia, from 2011 to 2012. He is currently an Associate Professor with Chongqing University. His current research interests include networked control systems, optimization of microgrids, evolutionary dynamics, and quantum games.

Congbo Peng received the B.S. degree in automation from Northwestern Polytechnical University, Xi'an, China, in 2014. He is currently an M.S. student with the School of Electrical Engineering, Chongqing University, Chongqing. His current research interests include multiagent systems and optimization of microgrids.

Minyou Chen (M'05–SM'14) received the M.Sc. degree in control theory and engineering from Chongqing University, Chongqing, China, in 1987, and the Ph.D. degree in control engineering from the University of Sheffield, Sheffield, U.K., in 1998. He is currently a Full Professor with Chongqing University. His current research interests include intelligent modeling and control, multiobjective optimization, micro-grid control, and state monitoring in power distribution systems.

Feixiong Chen received the B.S. degree in electrical engineering from Chongqing University of Technology, Chongqing, China, in 2012. He is currently pursuing the Ph.D. degree with the School of Electrical Engineering, Chongqing University, Chongqing. His current research interests include multiagent systems and optimization of microgrids.

Wenfa Kang received the B.S. degree in electrical engineering from Chengdu University of Information Technology, Chengdu, China, in 2014. He is currently an M.S. student with the School of Electrical Engineering, Chongqing University, Chongqing. His current research interests include networked control systems and optimization of microgrids.

Josep M. Guerrero (S'01–M'04–SM'08–F'15) received the B.S. degree in telecommunications engineering, the M.S. degree in electronics engineering, and the Ph.D. degree in power electronics from the Technical University of Catalonia, Barcelona, in 1997, 2000 and 2003, respectively. Since 2011, he has been a Full Professor with the Department of Energy Technology, Aalborg University, Denmark. His research interests are oriented to different microgrid aspects, including power electronics, hierarchical and cooperative control, energy management systems, and optimization of microgrids and islanded minigrids. Prof. Guerrero is an Associate Editor for the IEEE TRANSACTIONS ON POWER ELECTRONICS, the IEEE TRANSACTIONS ON INDUSTRIAL ELECTRONICS, and the IEEE INDUSTRIAL ELECTRONICS MAGAZINE, and an Editor for the IEEE TRANSACTIONS ON SMART GRID. He has been a Guest Editor of the IEEE TRANSACTIONS ON INDUSTRIAL ELECTRONICS SPECIAL SECTIONS: UNINTERRUPTIBLE POWER SUPPLIES SYSTEMS, etc. He was the chair of the Renewable Energy Systems Technical Committee of the IEEE Industrial Electronics Society.

Derek Abbott (M'85–SM'99–F'05) was born in South Kensington, London, U.K., in 1960. He received the B.Sc. (honors) degree in physics from Loughborough University, Leicestershire, U.K., in 1982 and the Ph.D. degree in electrical and electronic engineering from The University of Adelaide, Adelaide, S.A., Australia, in 1995, under K. Eshraghian and B. R. Davis. From 1978 to 1986, he was a Research Engineer at the GEC Hirst Research Centre, London, U.K. Since 1987, he has been with The University of Adelaide, where he is presently a full Professor with the School of Electrical and Electronic Engineering. His interest is in the area of multidisciplinary physics and electronic engineering applied to complex systems. His research programs span a number of areas including networks, game theory, energy policy, stochastics, and biophotonics. Prof. Abbott is a Fellow of the Institute of Physics (IOP) and Fellow of the Institute of Electrical & Electronic Engineers. Prof. Abbott has served as an Editor and/or Guest Editor for a number of journals including the IEEE JOURNAL OF SOLID-STATE CIRCUITS, PROCEEDINGS OF THE IEEE, the IEEE PHOTONICS JOURNAL, *PLOSONE,* and is currently on the editorial boards of Nature's *Scientific Reports*, IEEE ACCESS, *Royal Society Open Science* (RSOS), and *Frontiers in Physics.*